New Bidirectional Intelligent Semiconductor Transformer for Smart Grid Application

[1] Vaishnavi Sudhir Nakshane
P.G Student,
[1]Department Of Integrated Power System,
Abha Gaikwad Patil College Of Engineering, Nagpur, India.

Abstract: This paper proposes a new bidirectional intelligent semiconductor transformer (BIST) for the smart distribution system and smart grid. The proposed BIST consists of high-voltage high-frequency ac/dc converter, bidirectional low-voltage dc/dc converter, and hybrid-switching dc/ac inverter. It features 1) input-to-output isolation with a high-frequency transformer; 2) bidirectional power flow; 3) small size and light weight; 4) capability of compensating voltage sag and/or swell; and 5) realization of three-phase structure based on single-phase module. The operational feasibility of proposed transformer was verified not only by computer simulation with PSCAD/EMTDC software but also by a hardware prototype with rating of 1.9 kV/127 V, 2 kVA, allowing a three-phase transformer of 3.3 kV/220 V, 6 kVA with three-phase construction.

Index Terms - AC/DC resonant converter, bidirectional power flow, hybrid switching, input voltage balancing, intelligent semiconductor transformer (IST)

I. INTRODUCTION

CONVENTIONAL transformer composed of coil and iron core can change only the magnitude of the ac voltage and the quality of supplying power is totally dependent on that of the input power. So, it cannot be applicable for the smart grid, in which the magnitude and frequency of the operation voltage are various and high-quality power is required. Intelligent semiconductor transformer or solid-state transformer was proposed by EPRI to replace the conventional transformer in railway systems and substations, in which light weight is mandatorily required [1]. Recently, EPRI has reported 100 kVA single-phase semiconductor transformer named intelligent universal transformer for distribution automation [2]. Intelligent semiconductor transformer can easily offer small size and light weight because it operates at much higher frequency with reduction of the magnetic component. It can supply not only the dc power, but also high-quality ac power to the customer by compensating the voltage sag, swell, and harmonics. So, it can be utilized for implementing the smart distribution system and the micro grid [3]–[5]. Various kinds of intelligent semiconductor transformers were already proposed. However, since the power flow in these transformers is unidirectional, it is not properly applicable for the dc distribution and micro grid [1], [2], [6]–[10]. One can find some studies on the semiconductor transformer topologies with bidirectional power flow capability [11]–[23].

II. THEORETICAL FRAMEWORK

PROPOSED SEMICONDUCTOR TRANSFORMER

A. High-Voltage Part

Fig. 1 shows the power circuit of ac/dc rectifier, which converts single-phase ac voltage of 1900 V into full-bridge-rectified waveform of 320 V. The ac/dc converter has high-frequency transformers, which offer high-frequency resonance and input– output isolation. The input side works under high voltage, while the output side works under low voltage. So, the input side is designed with three half-bridge modules connected in series, in which two IGBT units are connected in series in the reverse direction. The output side is designed with three half-bridge modules connected in shunt. Whole system operates in bidirectional high-frequency resonance mode under a fixed frequency with 50% duty ratio to reduce system size and switching loss.

Because the resonant stage is basically an LLC converter, the input-to-output gain of each resonant converter, that is defined by vlink/|vac1|, is determined only by its transformer turns-ratio nT if the resonant frequency fr is equal to the switching frequency fsr [24], where vac1 is the input voltage of each resonant stage and it is equal to vac/3. Since the input and output filter capacitors of Cin and CL are much larger than Cr and parasitic capacitances of switches are much smaller than Cr, the resonant frequency fr, which is equal to fsr, is calculated as $1/[2\pi(2LrCr)0.5]$ with resonant inductor Lr and two resonant capacitors of Cr. Fig. 2 shows the switching pulses for each switch in a single-module of the bidirectional high-frequency ac/dc converter according to the polarity of the ac input voltage. The gating pulses for each switch are generated with same pattern regardless of the direction of power flow. Before explanation, it is assumed that the magnetizing inductance Lm is infinity.

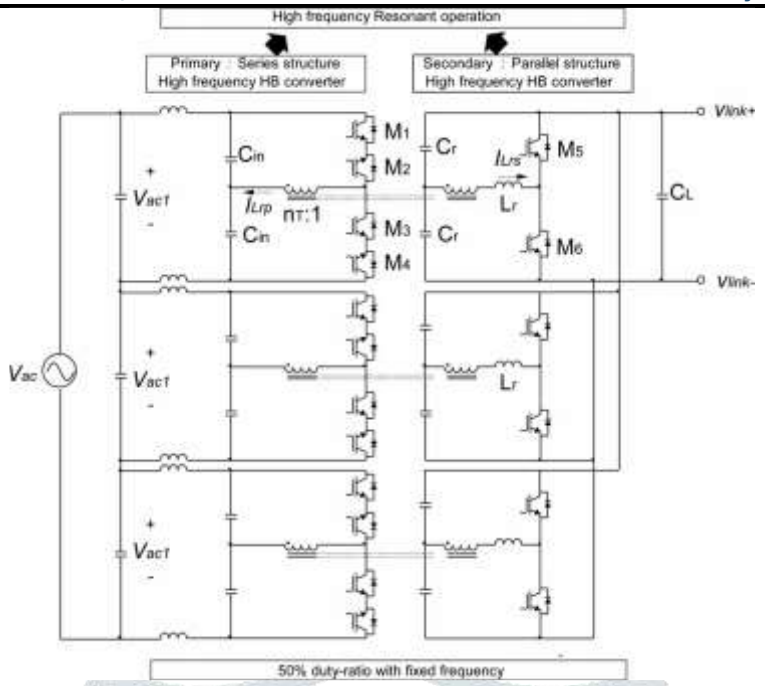

Fig 1

Mode 1: The direction of power flow is forward and the polarity of input voltage is positive. In the first stage, the primary current flows through the transistor in M1 and the diode in M2 when M1 turns ON. At this instance, the secondary current flows through diode in M5. In the next stage, the primary current flows through the transistor in M3 and the diode in M4 when M3 turns ON. At this instance, the secondary current flows through the diode in M6.

Mode 2: The direction of power flow is forward and the polarity of input voltage is negative. In the first stage, the primary current flows through the transistor in M2 and the diode in M1 when M2 turns ON. At this instance, the secondary current flows through diode in M6. In the next stage, the primary current flows through the transistor in M4 and the diode in M3 when M4 turns ON. At this instance, the secondary current flows through the diode in M5.

Mode 3: The direction of power flow is backward and the polarity of input voltage is positive. In the first stage, the secondary current flows through transistor in M5 when M5 turns ON. At this instance, the primary current flows through the diode in M1 and the transistor in M2. In the next stage, the secondary current flows through the transistor in M6 when M6 turns ON. At this instance, the primary current flows through the diode in M3 and the transistor in M4.

Mode 4: The direction of power flow is backward and the polarity of input voltage is negative. In the first stage, the secondary current flows through transistor in M6 when M6 turns ON. At this instance, the primary current flows through the transistor in M1 and the diode in M2. In the next stage, the secondary current flows through the transistor in M5 when M5 turns ON. At this instance, the primary current flows through the transistor in M3 and the diode in M4.

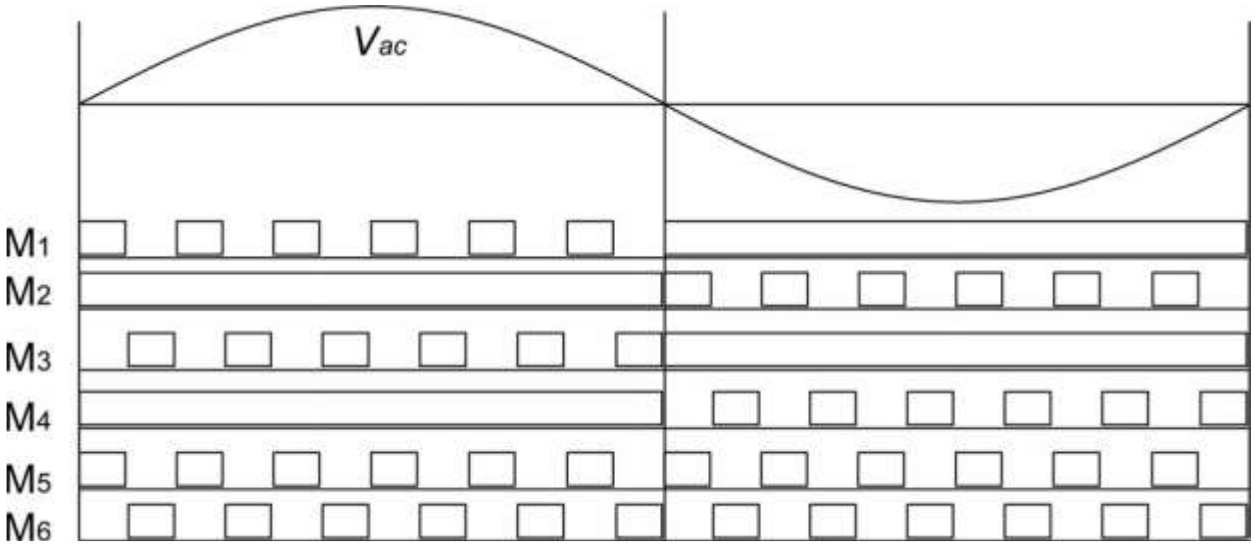

Fig 2

B. Low-Voltage Part

The low-voltage part consists of the dc/dc converter and the dc/ac inverter connected in cascade. The dc/dc converter changes the full-bridge rectified waveform of 320 V into the constant dc voltage of 700 V and the dc/ac inverter changes the constant dc voltage of 700 V into the single-phase ac voltage of 127 V. The dc/dc converter and dc/ac inverter use a hybrid switch with IGBT and MOSFET connected in parallel. The dc/dc converter and dc/ac inverter are composed of two half-bridges connected in cascade. The dc/dc converter operates to control the power factor and the dc-link voltage, while the dc/ac inverter operates to control the output voltage. As the switching frequency in IGBT increases, the switching loss increases due to tail-current, which critically reduces the system efficiency. In order to improve this switching loss, a MOSFET is connected in parallel to implement a hybrid switch. Fig. 3 shows how to supply the gating signal to the hybrid switch. The MOSFET turns ON a few microseconds ahead when the IGBT switch turns OFF. After the MOSFET turns ON, the IGBT turns OFF immediately and the MOSFET turns OFF at the instant that the IGBT is originally to turn OFF. Hybrid switching offers reduction of recovery loss due to tail-current. If a diode is connected in series with MOSFET, MOSFET destruction due to counter electromotive force can be protected. If resistance is connected in parallel with diode, ringing phenomenon can be reduced.

C. Zero-Voltage-Switching (ZVS) Operation

Since the magnetizing inductance Lm cannot have infinity value in real transformer, operational modes are somewhat different from that explained and it is helpful to achieve soft-switching of switches. All modes in Fig. 4 have same ZVS operation so that operational mode analysis is explained based on mode 1 of forward power flow with positive input voltage. Fig. 3 shows ZVS operation in mode 1 when the magnetizing inductance is not infinity. Before explanation, it is assumed that the resonant frequency fr is equal to the switching frequency fsr.

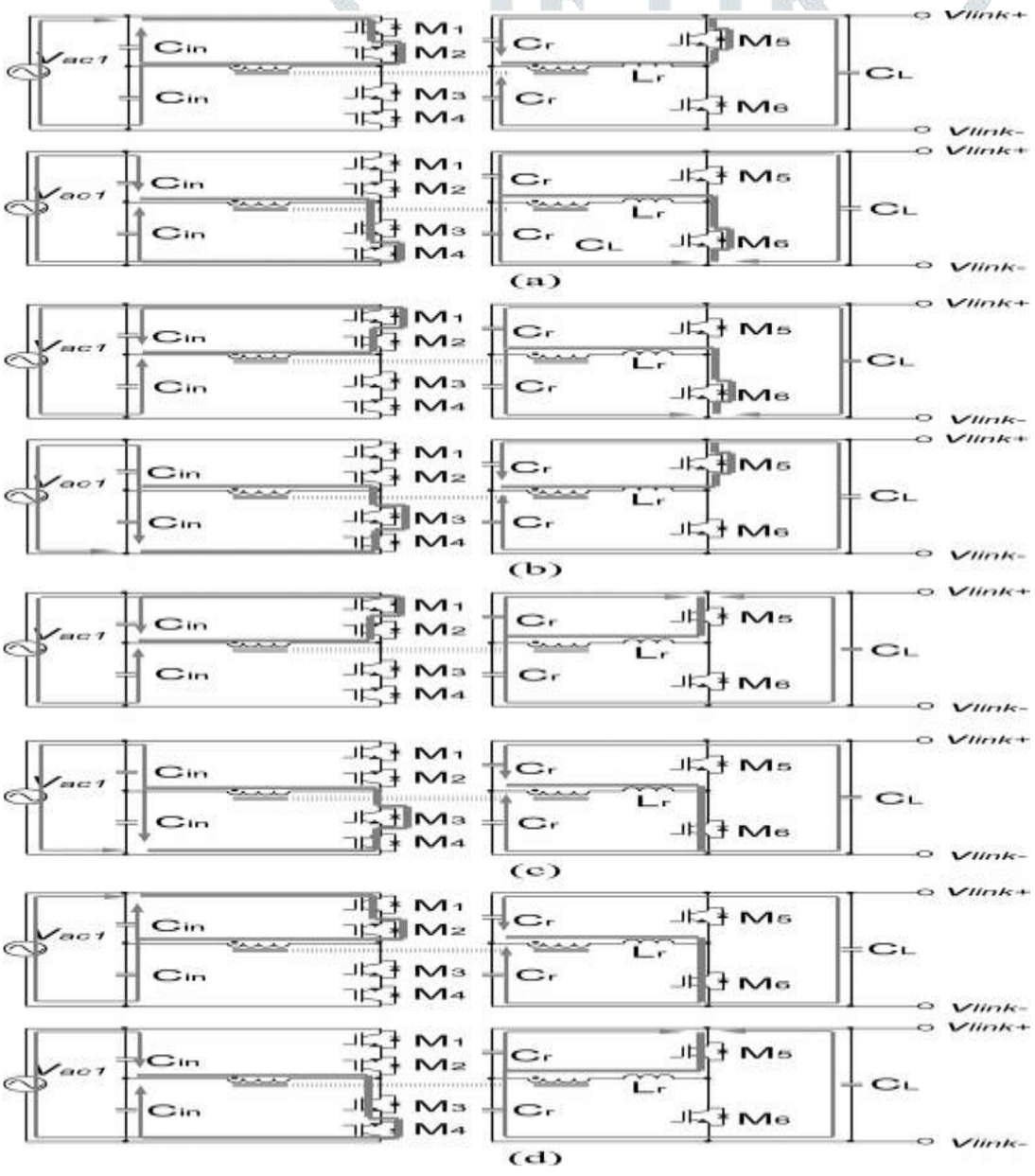

Fig 3

Mode A: The magnetizing current charges collector–emitter capacitance of M3Cce,M 3 and discharges collector–emitter capacitance of M1Cce,M 1 . Thus, collector–emitter voltage of M3vce,M 3 increases and collector–emitter voltage of M1vce,M 1decreases. When vce,M 3 exceeds the source voltage or vce,M 1crosses zero, the body diode of M1 starts to conduct the current. At this instant, the mode A starts. During mode A, the secondary resonant current iLrs begins to flow with resonant manner and it is divided into half and each half currents flow through the two resonant capacitors as shown in Fig. 3. The primary resonant current iLrp is the sum of the magnetizing current iM and secondary resonant referred to the primary side, which can be expressed as iLrs/nT . Since iLrs/nT is smaller than iM ,the primary resonant current iLrp is negative so that it flows through body diode in M1 and transistor in M2 from the negative peak value of the magnetizing current—IM,pk . This mode continues until iLrs/nT is equal to iM .

Mode B: After iLrs/nT is greater than iM ,iLrp flows through transistor in M1 and body diode in M2. Since the resonant frequency fr is equal to the switching frequency fsr,iLrs is nearly reduced to zero at the end of this mode.

Mode C: When M1 is turned OFF, only the magnetizing current remains on the primary side and it can be assumed that the magnetizing current is constant because mode C is a short dead-time period. As shown in Fig. 3, all switches of M1 and M3 are in turn-off state so that they can be modeled as their collector–emitter capacitances of Cce,M 1 and Cce,M 3 .

Accordingly, the magnetizing current flows through two paths of Lm ,Cin, collector–emitter capacitance of M1Cce,M 1 , body diode in M2 and Lm ,Cin, transistor in M4, collector–emitter capacitance of M3Cce,M 3 . Therefore, Cce, M 1 is charged from zero to vac1 by the half of the magnetizing current and Cce, M 3is discharged from vac1 to zero by the half of the magnetizing current. If mode C operation is completed before M3 is turnedON, ZVS of M3 can be accomplished. ZVS of M1 has the same manner as that of M3. Fig. 3 is computer simulation of ZVS operation in mode 1 of forward power flow with the positive input voltage. It shows that the simulation waveforms are similar to those shown in Fig. 3.

III. Topological Overview

The different components of a bidirectional DC–DC converter with galvanic isolation are depicted in Figure 4:

• The port 1 and port 2 filter networks provide smooth terminal voltages and currents. For each filter network, at least a single capacitor or a single inductor is employed.

• The DC–AC converter is a switch network which provides AC power to the HF transformer and the AC–DC converter supplies DC power to the receiving port; both converters must allow for bidirectional power

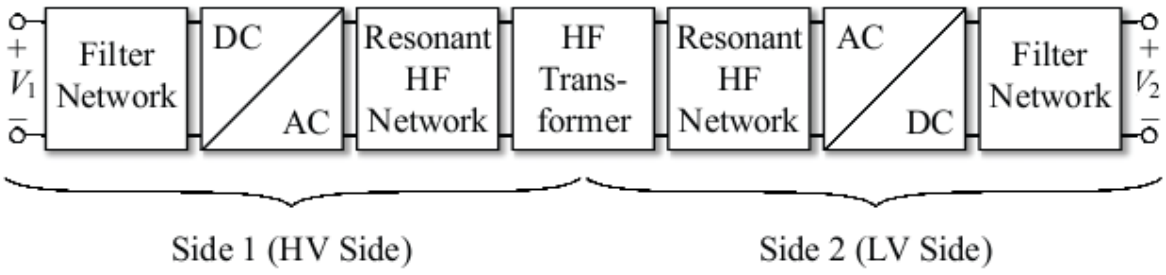

Fig 4: The different components required for an isolated, bidirectional DC-DC converter

transfer. Typically, full bridge circuits, half bridge circuits, and push-pull circuits are employed. However, different solutions (e.g. the single switch networks used in a bidirectional flyback converter) are reported, as well [41,42].

• The reactive HF networks provide energy storage capability within the HF AC part and are used to modify the shapes of the switch current waveforms in order to achieve low switching losses. Even though, these parts are not necessarily required for a fully functional bidirectional DC–DC converter, they will always be present in practice due to the parasitic components of the HF transformer (e.g. stray and magnetizing inductances, parasitic capacitances).

• The HF transformer is required in order to achieve electric isolation; it further enables large voltage and current transfer ratios. The HF transformer is considered superior over a low frequency transformer, since transformer and filter components become smaller (and often less expensive) at higher frequencies [35].2

Bidirectional DC–DC converter topologies with a system configuration according to Figure 4, are called Single-Stage Topologies [45, 46], since they contain a minimum number of conversion stages. Accordingly, the total number of required components is comparably low. However, the operation within wide input and output voltage ranges causes ineffective transformer and switch

utilization. Improved transformer and switch utilization is achieved with multi-stage topologies, which contain an additional power converter in order to adjust voltage and current levels.

3.1 Single-Stage Topologies

In the presented approach, single-stage topologies are grouped into

1. Converters with a low number of switches.

2. Dual bridge converters without resonant HF network, and

3. dual bridge converters with resonant HF network,

Assumptions	
Assumed efficiency at full load:	90%
Selected turns ratio $n = N_1 : N_2$:	19
Peak-to-peak current ripple, HV side:	$\leq$ 40% of full load DC curr.
Peak-to-peak current ripple, LV side:	$\leq$ 40% of full load DC curr. (selected in accordance to Appendix A.5.2)
HV side switches	
Peak voltage:	754 V
Peak current:	21.4 A
Max. RMS current:	14.6 A
VA rating:	11.0 kVA
LV side switches	
Peak voltage:	40 V
Peak current:	407 A
Max. RMS current:	258 A
VA rating:	10.2 kVA
Transformer	
Max. equiv. value of the HV side transf. voltage [cf. (B.5)]:	403 V
Max. HV side RMS current:	9.9 A
Max. equiv. value of the LV side transf. voltage [cf. (B.5)]:	21.2 V
Max. LV side RMS current:	189 A
VA rating:	4.0 kVA

HV side inductor	
Employed inductance:	920 µH
Peak current:	10.0 A
Peak energy:	46 mJ
LV side inductor	
Employed inductance:	1.7 µH
Peak current:	224 A
Peak energy:	43 mJ

Fig 5 : Cuk Converter topology: assumed specifications and result.

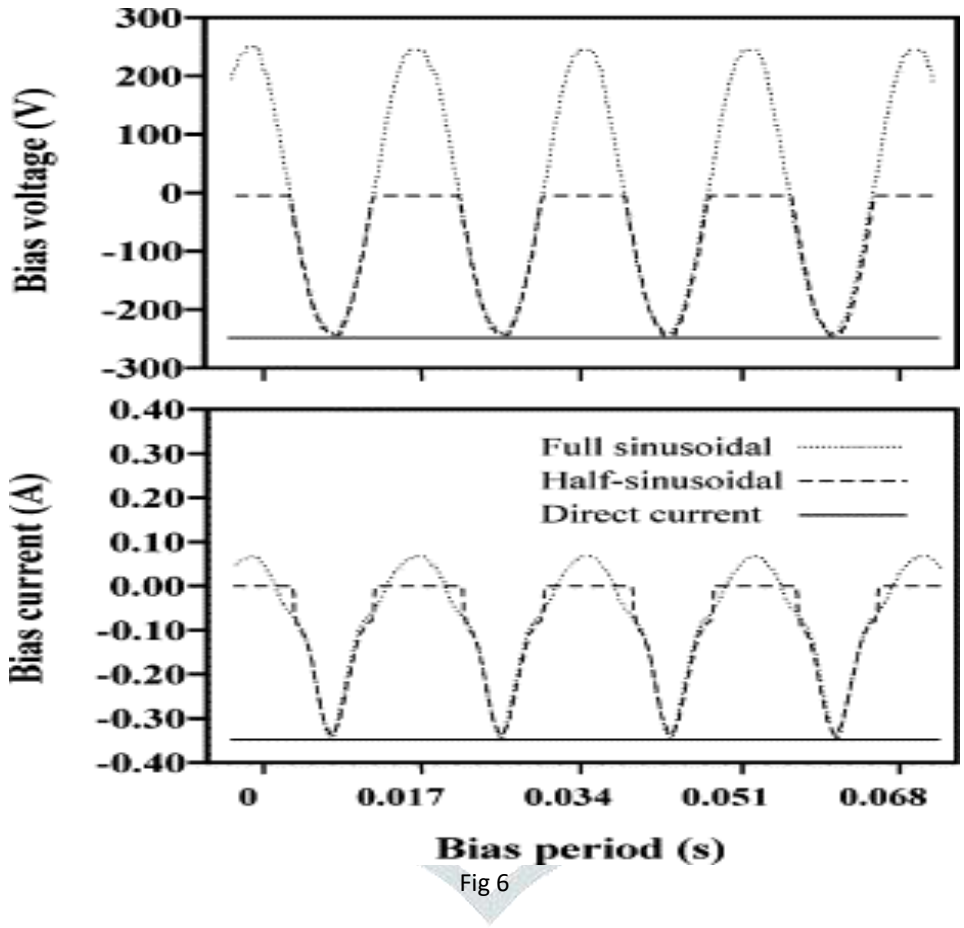

Fig 6

SIMULATION RESULTS AND OUTPUTS

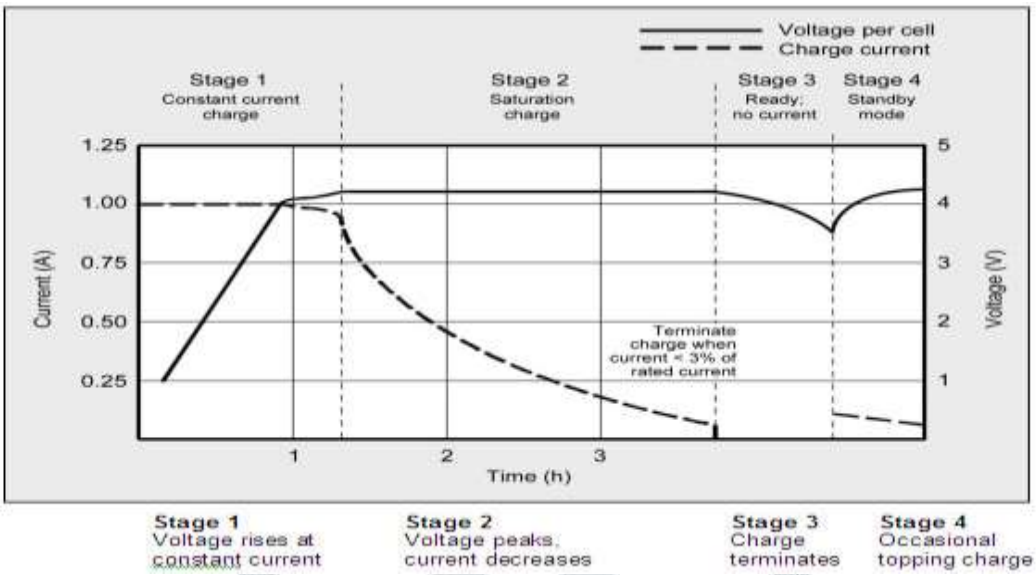

Fig 7

IV. CONCLUSION

In this paper, a new configuration of the BIST was proposed, which has rating of 1.9 kV/127 V, 2 kVA. The transformer consists of the high-voltage high-frequency ac/dc rectifier, and low-voltage dc/dc and dc/ac converters. The operational feasibility of the proposed transformer was verified by computer simulation with PSCAD/EMTDC software. Based on the simulation results, a hardware prototype with rating of 1.9 kV/127 V, 2 kVA was built and tested in the lab to confirm the feasibility of hardware implementation. Using three units of this transformer, a three-phase transformer with rating of 3.3 kV/220 V, 6 kVA can be built. The proposed transformer could be applicable for implementing the smart grid.

V. REFERENCES

[1] "Feasibility assessment for intelligent universal transformer," EPRI, Palo Alto, CA, USA, EPRI Rep. TR-1001698, Dec. 2002.

[2] M. Arindam, S. Ashok, G. Mahesh, B. Simon, and D. Shoubhik, "Intelligent universal transformer design and applications," in Proc. 20th Int. Conf. Exhib. Elect. Distrib., 2009, pp. 1–7.

[3] X. She, R. Burgos, G. Wang, F. Wang, and A. Q. Huang, "Review of solid state transformer in the distribution system: From components to field application," in Proc. IEEE Energy Convers. Congr. Expo., 2012, pp. 4077–4084.

[4] S. Falcones, R. Ayyanar, and X. Mao, "A DC–DC multiport-converter-based solid-state transformer integrating distributed generation and storage," IEEE Trans. Power Electron., vol. 28, no. 5, pp. 2191–2203, May 2013.

[5] G. Oritz, D. Bortis, J. W. Kolar, and O. Apledoorn, "Soft-Switching techniques for medium-voltage isolated bidirectional DC/DC converters in solid state transformers," in Proc. 38th Annu. Conf. IEEE Ind. Electron. Soc., 2012, pp. 5233–5240.

[6] L. Heinemann and G. Mauthe, "The universal power electronics based distribution transformer, an unified approach," in Proc. IEEE 32nd Annu. Power Electron. Spec. Conf., 2001, pp. 504–509.

[7] J. W. Merwe, T. Du, and H. Mouton, "The solid-state transformer concept: A new era in power distribution," in Proc. APRICON'90, 2009, pp. 1–6.

[8] E. Ronan, Jr., S. Sudhoff, S. Glover, and D. Galloway, "A power electronic-based distribution transformer," IEEE Trans. Power Deliv., vol. 17, no. 2, pp. 537–543, Apr. 2002.

[9] J. S. Lai, A. Maina, A. Mansoor, and F. Goodman, "Multilevel intelligent universal transformer for medium voltage applications," in Proc. Ind. Appl. Conf., 2005, pp. 1893–1899.

[10] T. Zhao, L. Yang, J. Wang, and A. Q. Huang, "270 kVA solid state transformer based on 10 kV SiC power devices," in Proc. IEEE Elect. Ship Technol. Symp., 2007, pp. 145–149.

[11] M. Kang, P. Enjeti, and I. Pitel, "Analysis and design of electronic transformers for electric power distribution system," IEEE Trans. Power Electron., vol. 14, no. 6, pp. 1133–1141, Nov. 1999.

[12] H. Qin and J. W. Kimball, "AC-AC dual active bridge converter for solid state transformer," in Proc. IEEE Energy Convers. Congr. Expo., 2009, pp. 3039–3044.

[13] E. C. Aeloiza, P. N. Enjeti, L. A. Moran, and I. Pitel, "Next generation distribution transformer: To address power quality for critical loads," in Proc. IEEE Annu. Power Electron. Spec. Conf., 2003, pp. 1266–1271.

[14] Z. Tiefu, Z. Jie, S. Bhattachaya, M. E. Baran, and A. Q. Huang, "An average model of solid state transformer for dynamic system simulation," in Proc. IEEE Power Energy Soc., 2009, pp. 1–8.

[15] X. She, A. Q. Huang, S. M. Lukic, and M. E. Baran, "On integration of solid-state transformer with zonal DC microgrid," IEEE Trans. Smart Grid, vol. 2, no. 2, pp. 975–985, Jun. 2012.

[16] H. Fan and H. Li, "High-Frequency transformer isolated bidirectional DC–DC converter modules with high efficiency over wide load range for 20 kVA solid-state transformer," IEEE Trans. Power Electron., vol. 26, no. 12, pp. 3599–3608, Dec. 2011.

[17] J. Shi, W. Gou, H. Yuan, T. Zhao, and A. Q. Huang, "Research on voltage and power balance control for cascaded modular solid-state transformer," IEEE Trans. Power Electron., vol. 28, no. 4, pp. 1523–1532, Apr. 2013.

[18] T. Zhoa, G. Wang, S. Bhattacharya, and A. Q. Huang, "Voltage and power balance control for a cascaded H-Bridge converter-based solid-state transformer," IEEE Trans. Power Electron., vol. 26, no. 4, pp. 1154–1166, Apr. 2011.

[19] S. H. Hwang, X. Liu, J. M. Kim, and H. Li, "Distributed digital control of modular-based solid-state transformer using DSP+FPGA," IEEE Trans. Ind. Electron., vol. 60, no. 2, pp. 670–680, Feb. 2013.

[20] X. Liu, H. Li, and Z. Wang, "A Start-Up scheme for a three-stage solid-state transformer with minimized transformer current response," IEEE Trans. Power Electron., vol. 27, no. 12, pp. 4832–4836, Dec. 2012.

[21] X. She, A. Q. Huang, and G. Wang, "3-D space modulation with voltage balancing capability for a cascaded seven-level converter in a solid-state transformer," IEEE Trans. Power Electron., vol. 26, no. 12, pp. 3778– 3789, Dec. 2011.

[22] G. Oritz, H. Uemura, D. Bortis, J. W. Kolar, and O. Apledoorn, "Modeling of soft-switching losses of IGBTs in high-power high-efficiency dual-active-bridge DC/DC converters," IEEE Trans. Electron. Devices, vol. 60, no. 2, pp. 587–597, Feb. 2013.

[23] G. Oritz, M. Leibl, J. W. Kolar, and O. Apledoorn, "Medium frequency transformers for solid-state-transformer applications—design and experimental verification," in Proc. 10th Int. Conf. Power Electron. Drive Syst., 2013, pp. 1285–1290.

[24] J. Y. Lee, Y. S. Jeong, and B. M. Han, "An isolated DC/DC converter using high-frequency unregulated LLC resonant converter for fuel cell applications," IEEE Trans. Ind. Electron., vol. 58, no. 7, pp. 2926–2934, Jul. 2011.

[25] B. Lu, W. Liu, Y. Liang, F. C. Lee, and J. D. van Wyk, "Optimal design methodology for LLC resonant converter," in Proc.

21st Annu. IEEE Appl. Power Electron. Conf. Expo., 2006, pp. 533–538.